DOI: https://dx.doi.org/10.4314/gjgs.v24i2.2

GLOBAL JOURNAL OF GEOLOGICAL SCIENCES VOL. 24, 2026: 203-215
COPYRIGHT© BACHUDO SCIENCE CO. LTD PRINTED IN NIGERIAISSN 1596-6798, e-ISSN: 2992–4502
www.globaljournalseries.com.ng, Email: globaljournalseries@gmail.com

COMPARATIVE STUDY OF AQUIFER SYSTEMS IN PARTS OF THE BASEMENT COMPLEX AND COASTAL PLAIN SANDS OF SOUTHEASTERN NIGERIA USING GEOPHYSICAL TECHNIQUES AND GEOCHEMICAL PARAMETERS

RITA A. ARCHIBONG, MFONISO U. AKA, EMMANUEL E. OKON, ANTHONY UGBAJA AND OKECHUKWU E. AGBASI

(Received 13 July 2026; Revision Accepted 4 August 2026)

ABSTRACT

This study presents the robust, multi-parameter comparative evaluation of the geophysical and geochemical characteristics of two distinct geological formations in Southeastern Nigeria. The fractured crystalline basement of the Southern Oban Massif (Awi Community) and the porous sedimentary media of the Nigeria Delta Basin (Calabar Municipal). Twenty (20) vertical electrical sounding (VES) points under Schlumberger array, and sixteen (16) groundwater samples were analyzed for the modeling of the groundwater potential, water quality and access irrigation suitability. The geoelectrical modeling delineates high yield, porous aquifers within the sedimentary gravel/sand units in Calabar at depths between 19 and 42.9 m, in contrasts with structurally controlled, weathered to fractured regolith units in Awi. The geochemical analysis of the two formation depicts a host freshwater (TDS < 500 mg/l). Aquifers of both formations suffer from severe geogenic iron contamination up to 5.18mg/l and widespread anthropogenic nitrate loading exceeding the 50mg/l standard. The evaluated water quality through the weight arithmetic water quality index (WQI) yielded values consistently exceeding 300, classifying the untreated groundwater across both formations as unsuitable for direct consumption. Irrigation indices calculated for water samples from both formations presented a critical divergence; low sodium adsorption ratio (SAR) values suggested chemical safety, whereas highly elevated magnesium adsorption ratio (MAR) scores of up to 76.4 % posed a severe long-term risk of soil alkalization and structural degradation. Gibbs and Piper diagram visualization confirmed a transitional lifecycle in Calabar from precipitation-dominated to rock-water interaction-dominated facies, while Awi basement remains tightly cluster within the precipitation- dominated facies regime. Both aquifer systems are characterized by a highly mineralized Ca-Mg-Cl-SO water type, highlighting permanent hardness.

KEYWORDS: Aquifers, Groundwater, Oban Massif, Niger Delta Basin, Water Quality

INTRODUCTION

Groundwater is a vital source of potable water, particularly in regions where surface water resources are scarce.

The Niger Delta Basin encompasses diverse aquifer systems of Eocene to Recent Coastal Plain Sands, which transition into the weathered regolith and

Rita A. Archibong, Department of Geology, University of Calabar, Nigeria
Mfoniso U. Aka, Department of Physics, Federal University of Technology Ikot Abasi, Nigeria
Emmanuel E. Okon, Department of Geology, University of Calabar, Nigeria
Anthony Ugbaja, Department of Geology, University of Calabar, Nigeria
Okechukwu E. Agbasi, Department of Physics, Federal University of Technology Ikot Abasi, Nigeria

fractured rock units of the Precambrian Basement Complex of the Oban Massif, precisely within the Awi Community and its environs. Despite the strategic socio-economic importance of these hydrogeological units, comprehensive comparative studies of their hydrogeophysical, geochemical, and hydraulic properties using modern integrated techniques have remained limited.

The integrity of global freshwater resources faces unprecedented pressure due to the confluence of escalating human development, industrial expansion, and climatic uncertainty (Doherty, 2017). Across much of the developing world, and particularly within the Nigerian socio-economic landscape, groundwater has transitioned from a supplemental source to the primary, non-negotiable lifeline for domestic, agricultural, and industrial sustenance (Federal Ministry of Water Resources, FMWR, 2016). In the absence of robust, centralized water infrastructure, unconfined and shallow aquifers have become the default choice for millions, leading to the rapid and often unregulated development of boreholes and hand-dug wells. This phenomenon, while addressing immediate water needs, simultaneously places the aquifer systems at extreme risk of contamination. Subsurface water, characterized by its long residence time and slow flow velocity, is exceptionally vulnerable to long-term degradation from both naturally occurring geogenic processes and high-density, localized anthropogenic contamination (Ikechukwu & Ogbaji, 2019).

According to (Amah 2007), Groundwater serves as the primary source of drinking water in Calabar and surrounding areas in southeastern Nigeria. Numerous boreholes have been constructed by private companies, individuals, and government bodies such as the Cross River State Water Board (CRSWB) and the Rural Water Supply and Sanitation Agency (RUWASSA) to meet the growing water demand. However, many of these boreholes were developed without thorough geological, hydrogeological, or technical assessments, often relying on speculative configurations. This lack of systematic planning has contributed significantly to the high incidence of borehole failures in the region, keeping the availability of clean, reliable water critically low.

The successful exploration and sustainable management of this groundwater resource, particularly in geologically complex environments like the Nigerian Basement Complex and Coastal Plain Sands, remain a significant challenge (Jimoh et al., 2023). Groundwater occurrence in hard-rock terrains is primarily controlled by secondary porosity structures, specifically weathered basements, joints, and fractured zones, whereas sedimentary settings are dominated by primary intergranular porosity (Abubakar & Auwal, 2012; Ojo et al; 2024).

The delineation of these weathered fractured basement and costal sand aquifer systems requires non-invasive and cost-effective exploratory techniques, with surface geophysical methods being preferred for their ability to gather subsurface information without destructive action. Concurrently, the potability of this resource is paramount, as contamination can occur from surface infiltration, particularly in areas with poor protective overburden capacity. Therefore, a holistic approach integrating both geophysical techniques for resource mapping and physicochemical analysis for quality assessment is essential for effective groundwater resource development and management (Okorobia et al 2020 Amah et al., 2012).

Geophysical methods, particularly the Electrical Resistivity Method (ERM), offer a non-invasive means of characterizing the subsurface, delineating potential aquifer zones, and identifying pathways for contaminant migration (Oguamaetal 2019; Omosuyi 2010). Concurrently, a rigorous assessment of groundwater quality through physicochemical analysis is essential to ensure the water's suitability for human consumption and agricultural use, especially as dissolved solids, nitrates, and heavy metals pose serious public health risks (Patil et al 2012; Thomas, 2023). This research integrates the Vertical Electrical Sounding (VES) technique with hydrochemical analysis to provide a comprehensive, comparative evaluation of the subsurface structure and groundwater quality across these two hydrogeological settings.

DESCRIPTION OF THE STUDY AREA

The study area lies within latitudes 4°48'N and 5°20'N and longitudes 8°10'E and 8°30'E in southeastern Nigeria (Fig. 1). The Awi community is situated on the southern margin of the Precambrian Oban Massif (Ekwueme & Okoro, 2019). The local basement complex is dominated by gneisses and schists intercalated with low-silica, iron-, magnesium-, and calcium-rich amphibolite bands (Oden et al 2019). The adjacent Calabar Municipality sits entirely on the sedimentary Coastal Plain Sands (Benin Formation) (Olim et al 2020), an Eocene-to-Recent sequence characterized by thick, poorly-sorted, cross-bedded sand bodies interbedded with localized clay lenses. The regional hydrology is driven by a tropical wet-and-dry climate. Peak precipitation occurs during the wet season (including August), generating substantial surface run-off across networks of streams and rivers that drain towards the Cross River Basin. In the Awi Basement, primary porosity is negligible. Groundwater occurrence is restricted to the weathered overburden (saprolite) and underlying fractured bedrock (saprock).

In Calabar, the Coastal Plain Sands form a highly permeable unconfined-to-semi-confined porous aquifer system with high transmissivity, though its shallow water table makes it exceptionally sensitive to seasonal rainfall recharge and surface-derived contamination.

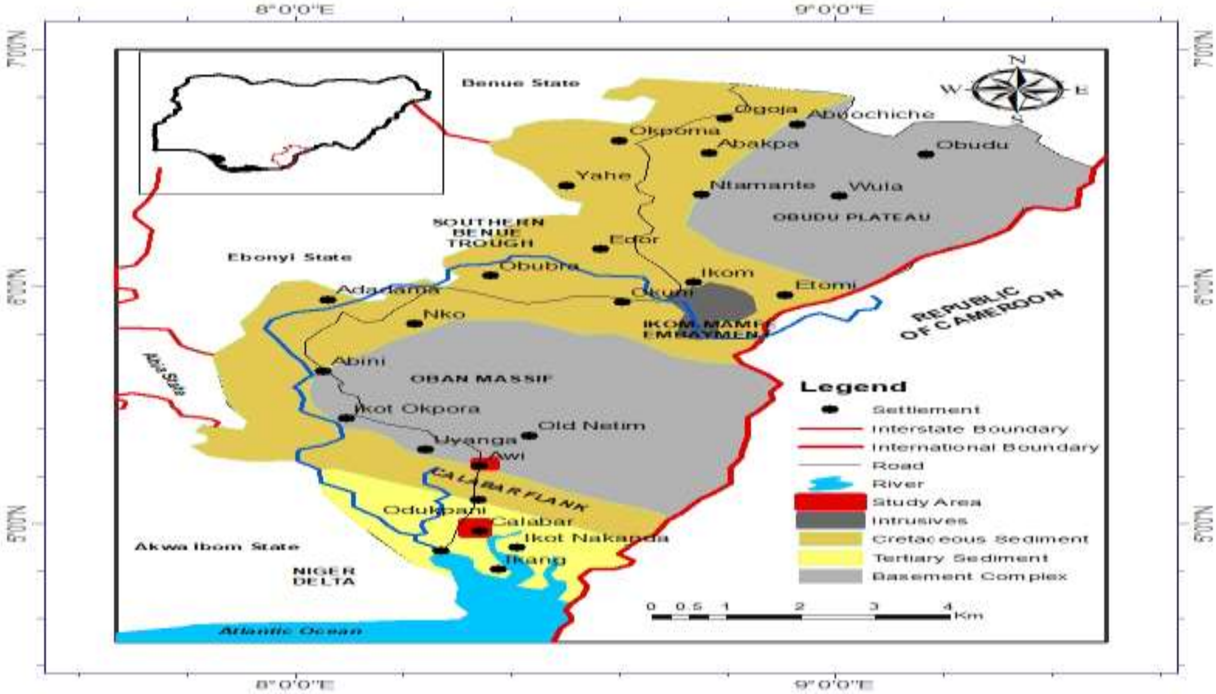

Fig. 1: Geologic Map of Cross River Showing the Study Area (Modified from Edet et al., 2011)

METHODOLOGY

Geoelectrical Parameters

A total of twenty (20) Vertical Electrical Sounding (VES) surveys were conducted using the Schlumberger electrode configuration. Ten soundings were situated in Calabar (VES 1 to 10), and ten in Awi (VES 11 to 20) respectively (Fig. 2). Global Positioning System (GPS) devices were used to record the spatial coordinates and elevation of each point. The data acquisition took place during the rainy season in August 2025.The current electrode half-spacing (AB/2) ranged from 1– 250 m, while the potential electrode half-spacing MN/2 varied from 0.5 – 30 m. The apparent resistance measurements were collected using an ABEM Terrameter SAS 300B. Thus, apparent resistivity (ρa) were calculated using standard geometric factors as shown in the equation (1):

$$\rho a = GR \tag{1}$$

The geometric factor G for the Schlumberger array is expressed as:

$$G = \pi \frac{(AB/2)^2 - (MN/2)^2}{MN} \tag{2}$$

The field curve data were plotted on bi-logarithmic papers and subjected to 1-D computer inversion modeling using IP2Win software to resolve the resistivity (ρa), thickness (H), and depth (D) of successive geoelectric layers, with minimal root mean square (RMS) errors (ranging between 0-10.5 %.

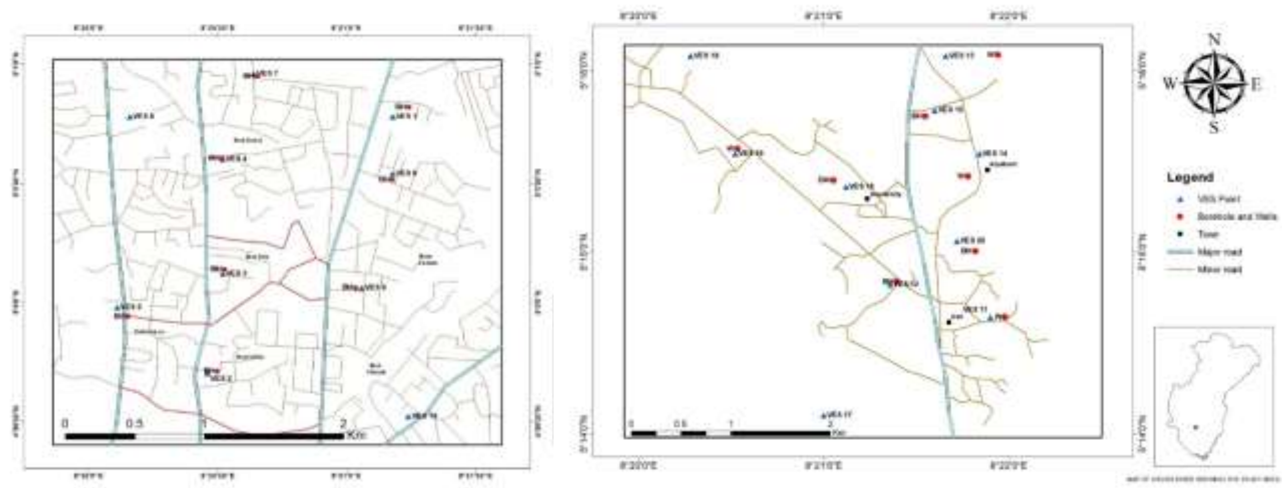

Fig. 2: VES points and water sample location in Calabar and Awi

Laboratory Analysis

Sixteen (16) groundwater samples were analyzed: Eight (8) each from Calabar and Awi boreholes. The samples were collected in clean, pre-rinsed 1.5 L polyethylene bottles. Physical parameters, including temperature, pH, and electrical conductivity (EC), were measured in the field using pre-calibrated portable meters. The samples were stored in a special box and transported for analyzes at the University of Uyo Biochemistry Laboratory. Major cations analyzed include Sodium (Na^+), Potassium (K^+), Calcium (Ca^{2+}), Magnesium (Mg^{2+}), and Total Dissolved Solid (TDS), Iron (Fe) and, major anions, Chloride (Cl^-). Sulphate (SO_4^{2-},), Nitrate (NO_{3-}), and Bicarbonate (HCO^-), were determined with high-precision spectrophotometry and standard titration methods in compliance with WHO (2011) protocols.

Geochemical Parameters

Water quality index (WQI)

A weighted arithmetic index was employed to calculate the overall water quality status: where the concentration of each parameter (*Ci)* in mg/L is divided by the corresponding WHO standard (*Si)* to derive a quality rating scale (*qi*). This ratio (*Ci/Si*) is then multiplied by a factor of 100, forming a mathematical expression as presented below:

$$qi = \frac{Ci}{Si} \times 100 \qquad (3)$$

The relative weight (*Wi*) is calculated as:

$$Wi = \frac{1}{Si} \qquad (4)$$

The final composite WQI is expressed as:

$$WQI = \Sigma qiwi \qquad (5)$$

Sodium Adsorption Ratio (SAR)

Sodium Adsorption Ratio (SAR) is an indicator that quantifies the amount of sodium (Na) in relation to calcium (Ca) and magnesium (Mg) in water extracted from saturated soil paste. It is calculated by dividing the Na concentration by the square root of half the combined Ca and Mg concentration (Reeve *et al.,* 1954). The suitability of water resources for irrigation is mainly determined by the Na concentration compared to the total concentration of Ca and Mg (Hem, 1985). As per the SAR hazard chart developed by the Agricultural Council of America, water is considered suitable for irrigation if it has an SAR value < 3 meq/L. The SAR was calculated using

$$SAR = \frac{Na^{2+}}{\sqrt{Ca^{2+} + Mg^{2+}}} \qquad (6)$$

Magnesium Adsorption Ratio (MAR)

Paliwal (1972) and Haritash *et al.,* (2016) highlighted that the Magnesium Adsorption Ratio (MAR) is an essential chemical factor to consider before utilizing a water resource for irrigation. They explained that the phenomenon indicates an unfavorable balance between calcium (Ca) and magnesium (Mg). When this imbalance occurs, the soil tends to become more alkaline, leading to a decline in soil quality, which in turn results in reduced crop yields (Haritash *et al.,* 2016). MAR is defined by the following equation, represented in meq/L.

$$MAR = \frac{Mg^{2+}}{Ca^{2+} + Mg^{2}+} \text{ X } 100 \qquad (8)$$

Statistical Analysis

Multivariate statistical analyses, including Pearson's correlation matrices, Principal Component Analysis (PCA), and Hierarchical Cluster Analysis (HCA), were executed using Past4 and Microsoft Excel to evaluate the factors controlling groundwater chemistry. PCA reduces the dimensionality of the physicochemical dataset using eigenvalue decomposition of the correlation matrix:

$$Cv = \lambda v \qquad (7)$$

Where *C* is the correlation matrix of the variables, λ is the eigenvalue, and *v* is the eigenvector representing each principal component. Components with eigenvalues greater than 1.0 were retained (Kaiser Criterion), and varimax rotation was applied to enhance interpretability.

RESULTS AND DISSCUSSION

The findings from the VES survey were conducted at both the Calabar sedimentary and Awi basement terrains. The parameters analyzed were apparent resistivity, depth, thickness as shown in Table. 1 and 2. However, Figures 3 and 4, shows the computer modeling of VES layers.

Table 1: VES parameters and characterization in Calabar Municipal

Longitude/latitude	VES	No. of Layers	Curve Type	Resistivity	Thickness	Depth	Lithology
8°21'12"/ 5°0'47"	1	4	HK	434.4	1.91	1.91	Top Layer compacted sand
				20.3	1.91	3.83	clayey sand
				1387	8.54	12.4	Gravel
				0.139	∞	∞	clay
8°20'27"/ 4°59'41"	2	4	HK	37.7	1.77	1.77	Top layer clayey sand
				6.14	2.94	4.71	clay
				1288	7.45	12.2	Gravel
				0.408	∞	∞	clay
8°20'28"/ 5°0'1"	3	4	KH	27.1	7.07	7.07	Top layer clayey sand
				206	5.53	12.6	coarse sand
				41.9	56.9	69.5	fine sand
				342	∞	∞	Gravel
8°20'30"/ 5°0'36"	4	4	KH	39.3	14.3	14.3	Top layer clayey sand
				705	6.62	20.9	coarse sand
				9.17	12.7	33.6	clay
				14495	∞	∞	Gravel
8°20'4.56"/ 5°0'10.26"	5	5	HKQ	86.8	0.462	0.462	Top layer compacted sand
				30.2	1.13	1.59	clayey sand
				65.5	14.6	16.2	fine sand
				536	26.7	42.9	Gravel
				1.04	∞	∞	clay
8°21'10"/ 5°0'32"	6	5	KHK	272	3.1	3.1	Top layer compacted sand
				50	1.25	4.35	clayey sand
				829	1.24	5.59	Gravel
				71.2	37.4	43	fine sand
				73.2	∞	∞	fine sand
8°20'38"/ 5°0'56"	7	4	HK	55.6	0.699	0.699	Top layer clayey sand
				16.1	5.44	6.14	clay
				2138	10.9	17.1	Gravel
				0.865	∞	∞	clay
8°29'09"/ 5°0'46"	8	4	HA	43.1	0.47	0.47	Top layer clayey sand
				8.07	0.534	1	clay
				139	32.1	33.1	coarse sand
				15343	∞	∞	Gravel
8°21'00"/ 5°0'09"	9	4	KQ	6.28	0.328	0.328	Top layer clayey sand
				1033	7.04	7.37	Gravel
				428	2.14	9.51	coarse sand
				4.78	∞	∞	clay
8°21'16"/ 4°58'9.20"	10	4	AK	14.9	0.306	0.306	Top layer clayey sand
				163	2.31	2.62	medium sand
				48627	1.84	4.46	gravel
				46.1	∞	∞	fine sand

Table 2: VES parameters and characterization in Awi

Longitude/Latitude	VES	No. of Layers	Curve Type	Resistivity	Thickness	Depth	Lithology
8°21'47"/ 5°14'40"	11	4	KH	58.3	18.1	18.1	overburden (clayey sand)
				347	10.6	28.6	weathered bedrock
				14.4	21.2	49.8	fractured bedrock
				22070	∞	∞	fresh bedrock
8°21'20"/ 5°14'40"	12	5	KHK	22.1	0.868	0.868	overburden (clayey sand)
				226	1.36	2.23	weathered bedrock
				15.9	2.01	4.23	fractured bedrock
				812	6.11	10.3	partially weathered bedrock
				130	∞	∞	fractured bedrock
8°21'41"/ 5°18'05"	13	4	KQ	250	0.315	0.315	overburden (Lateritic sand)
				2012	24.8	25.1	partially weathered bedrock
				292	15.8	40.9	Weathered/fractured basement rock
				2.30E+05	∞	∞	fresh bedrock
8°21'51"/ 5°5'31"	14	4	KQ	332	1.22	1.22	overburden (Lateritic sand)
				23107	1.39	2.61	partially weathered bedrock
				598	83.2	85.8	Fractured basement rock
				2.00E+05	∞	∞	fresh bedrock
8°21'35"/ 5°15'47"	15	5	HAK	3014	0.368	0.368	overburden (lateritic sand)
				207	0.522	0.89	weathered bedrock
				1516	26.4	27.2	partially weathered bedrock
				12109	24.9	52.1	fresh bedrock
				18.9	∞	∞	Mineralized bedrock
8°21'06"/ 5°15'23"	16	5		518	2.52	2.52	overburden (compacted sand)
				4143	1.64	4.16	partially weathered bedrock
				344	6.99	11.2	weathered bedrock
				1.20E+05	10.6	21.8	fresh bedrock
				994	∞	∞	fresh bedrock
8°20'59"/ 5°14'05"	17	4	QQ	2643	9.35	9.35	overburden (Lateritic sand)
				985	31	40.4	partially weathered bedrock
				267	22.3	62.7	Weathered/fractured bedrock
				1.30E+05	∞	∞	fresh bedrock
8°20'17"/ 5°16'06"	18	6	AKHK	136	0.21	0.21	overburden (compacted sand)
				2837	4.09	4.3	partially weathered bedrock
				51707	1.48	5.77	fresh bedrock
				1618	9.73	15.5	fresh bedrock
				77255	16.8	32.3	fresh bedrock
				464	∞	∞	fractured bedrock
8°20'32"/ 5°15'34"	19	4	KH	1415	3.372	3.372	overburden (lateritic sand)
				11789	1.765	5.137	fresh bedrock
				1534	139.6	144.7	fresh bedrock
				614378	∞	∞	fresh bedrock
8°21'43.52"/ 5°15'3.43"	20	3	A	24.26	0.1182	0.1182	overburden (clayey sand)
				315.2	43.56	43.68	weathered bedrock
				58961	∞	∞	fresh bedrock

Results of the physical parameters analyzed include temperature, pH, EC, TDS, salinity alongside other geochemical and statistical parameters of the water sample compared with WHO (2011) Standards, as shown in Table 3 to 4.

Table 3: Result of Physical and Geochemical Analysis of Water Samples in Calabar

PARAMETERS/LOCATION	L1	L2	L3	L4	L5	L6	L7	L9	WHO 2011
Temp 0ºC	26.4	26.2	26	26.1	26.5	26.1	26.2	26.3	32
pH	6.08	6.22	8.5	8.5	8.9	8.4	6.2	8.17	6.50 - 8.50
Salinity %	0	0	0.01	0.01	0.01	0.01	0	0.01	
Conductivity µscm-1	61.4	53.6	254	127.3	112.1	107.6	79	103.6	1500
Total dissolved solid mg/l	30.4	26.8	127.4	63.1	55.4	53.7	40	57.7	1000
(HCO_3) mg/l	76.00	48.00	112.00	88.00	89.60	56.00	74.40	76.00	100
Chloride (Cl-) mg/l	31.24	25.56	42.60	45.44	65.20	38.40	19.88	22.72	250.00
Nitrate (NO_3-) mg/l	25.37	54.16	90.98	88.36	35.96	67.91	45.06	62.88	50
Sulphate (SO_4^2-) mg/l	9.32	15.83	13.00	17.19	10.18	11.04	9.75	12.57	250
Calcium (Ca) mg/l	60.74	73.53	34.16	40.00	34.25	32.61	38.42	51.78	75
Magnesium (Mg) mg/l	49.12	42.60	67.34	61.15	60.12	51.30	40.63	54.50	50.00
Sodium (Na) mg/l	60.33	46.58	71.27	75.48	98.31	64.54	29.68	40.86	200
Potassium (K) mg/l	10.10	8.47	7.86	9.08	11.35	12.14	13.68	8.93	12
Iron (Fe) mg/l	3.77	1.73	1.83	1.88	3.87	2.51	1.99	1.94	0.3

Table 4: Result of Physical and Geochemical Analysis of Water Samples in Awi

PARAMETERS/LOCATION	L11	L12	L13	L14	L15	L16	L19	L20	WHO 2011
Temp 0ºC	26.1	26.2	25.9	26.1	26.1	26.2	26.1	7.01	32
pH	7.26	8.37	5.96	6.16	5.85	6.25	8.18	26.1	6.50 - 8.50
Salinity %	0	0.01	0	0	0	0	0.01	0	
Conductivity µscm-1	95.9	111.1	91.6	41.8	39.5	89.7	107.9	0	1500
Total dissolved solid mg/l	47.8	55.5	45.9	21	20.1	45	53	50.3	1000
(HCO_3) mg/l	104.00	48.00	32.00	64.00	48.00	80.00	84.01	101	100
Chloride (Cl-) mg/l	34.08	36.40	28.40	31.24	14.20	28.40	25.56	37.12	250.00
Nitrate (NO_3-) mg/l	82.31	80.37	32.41	53.20	56.23	41.96	45.90	85.31	50
Sulphate (SO_4^2-) mg/l	25.15	12.06	13.26	11.29	28.17	11.80	13.00	28.15	250
Calcium (Ca) mg/l	50.86	49.55	61.20	40.77	84.60	53.59	32.76	53.91	75
Magnesium (Mg) mg/l	49.78	55.16	48.39	33.43	40.61	39.89	64.22	52.56	50.00
Sodium (Na) mg/l	56.91	61.54	54.71	47.84	30.93	44.87	39.90	58	200
Potassium (K) mg/l	7.38	7.90	11.24	6.28	10.13	12.10	7.49	10.01	12
Iron (Fe) mg/l	1.94	1.88	2.19	5.18	2.67	2.04	2.35	4.94	0.3

Table 5: Water Quality Index (WQI) of Borehole/Hand-dug Wells

	Location	Σqiwi	Σwi	WQI	Classification
CALABAR	L1	4300.28	3.53	1218.33	Unsuitable
	L2	2057.14	3.53	582.81	Unsuitable
	L3	2100.96	3.53	595.23	Unsuitable
	L4	2166.51	3.53	613.80	Unsuitable
	L5	4365.35	3.53	1236.76	Unsuitable
	L6	2852.04	3.53	808.02	Unsuitable
	L7	2283.18	3.53	646.86	Unsuitable
	L9	2252.68	3.53	638.21	Unsuitable
AWI	L11	2251.77	3.53	637.96	Unsuitable
	L12	2182.77	3.53	618.41	Unsuitable
	L13	2545.68	3.53	721.22	Unsuitable
	L14	5831.86	3.53	1652.24	Unsuitable
	L15	3121.23	3.53	884.28	Unsuitable
	L16	2365.62	3.53	670.21	Unsuitable
	L19	2674.15	3.53	757.62	Unsuitable
	L20	5590.77	3.53	1583.94	Unsuitable

Table 6: Irrigation suitability parameter

	Location	SAR (meq/l)	MAR (%)	Soil Hazard / Suitability
CALABAR	L1	1.973	57.146	Low Sodium Hazard / Extremely High Magnesium Hazard
	L2	1.513	48.858	Low Sodium Hazard / Permissible Magnesium Level
	L3	2.303	76.474	Low Sodium Hazard / Severe Permeability Damage Risk
	L4	2.477	71.598	Low Sodium Hazard / Severe Permeability Damage Risk
	L5	3.315	74.323	Moderate Sodium Hazard / High Magnesium Hazard
	L6	2.322	72.176	Low Sodium Hazard / High Magnesium Hazard
	L7	1.126	63.554	Low Sodium Hazard / High Magnesium Hazard
	L9	1.337	63.445	Low Sodium Hazard / High Magnesium Hazard
AWI	L11	1.922	61.744	Low Sodium Hazard / High Magnesium Hazard
	L12	2.022	64.735	Low Sodium Hazard / High Magnesium Hazard
	L13	1.794	56.594	Low Sodium Hazard / High Magnesium Hazard
	L14	1.903	57.485	Low Sodium Hazard / High Magnesium Hazard
	L15	0.978	44.182	Low Sodium Hazard / Permissible Magnesium Level
	L16	1.599	55.105	Low Sodium Hazard / High Magnesium Hazard
	L19	1.32	76.373	Low Sodium Hazard / Severe Permeability Damage Risk
	L20	1.905	61.652	Low Sodium Hazard / High Magnesium Hazard

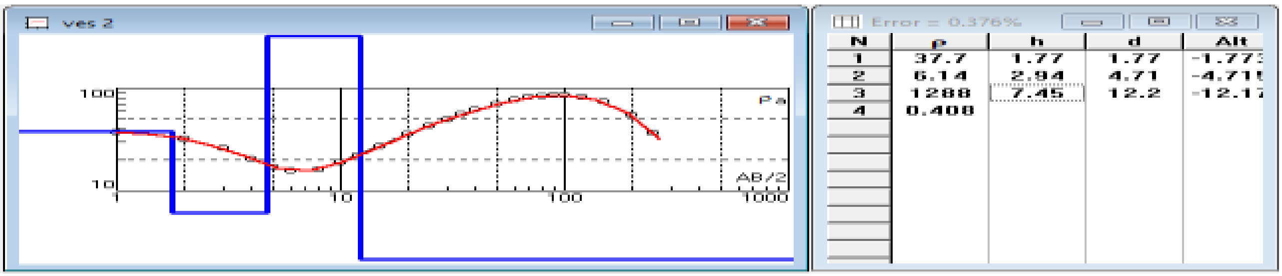

Fig.3: Computer modeled curve of VES and layer in Calabar

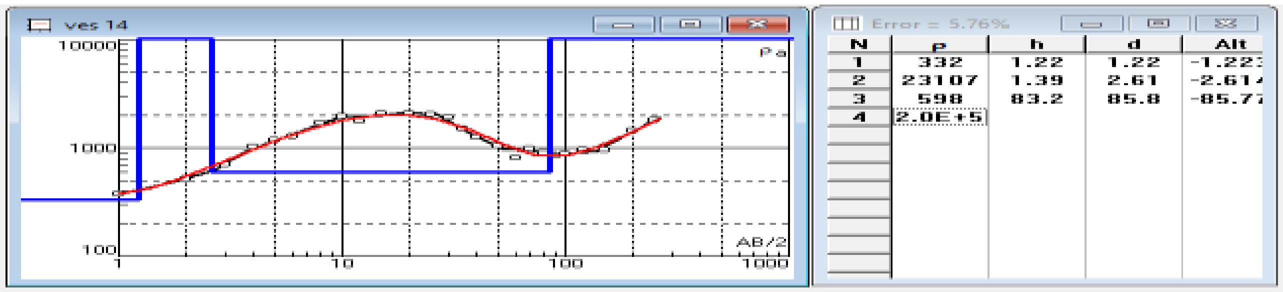

Fig.4: Computer modeled curve of VES and layer in Awi

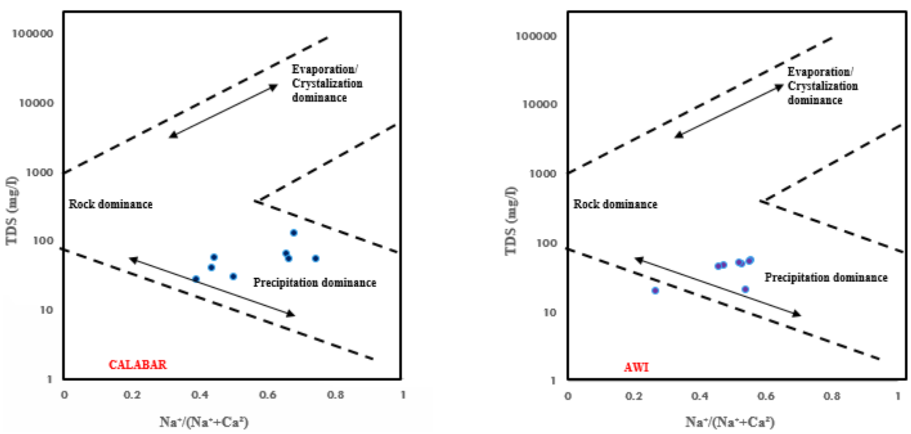

Fig. 5: Gibb's plot of Calabar and Awi

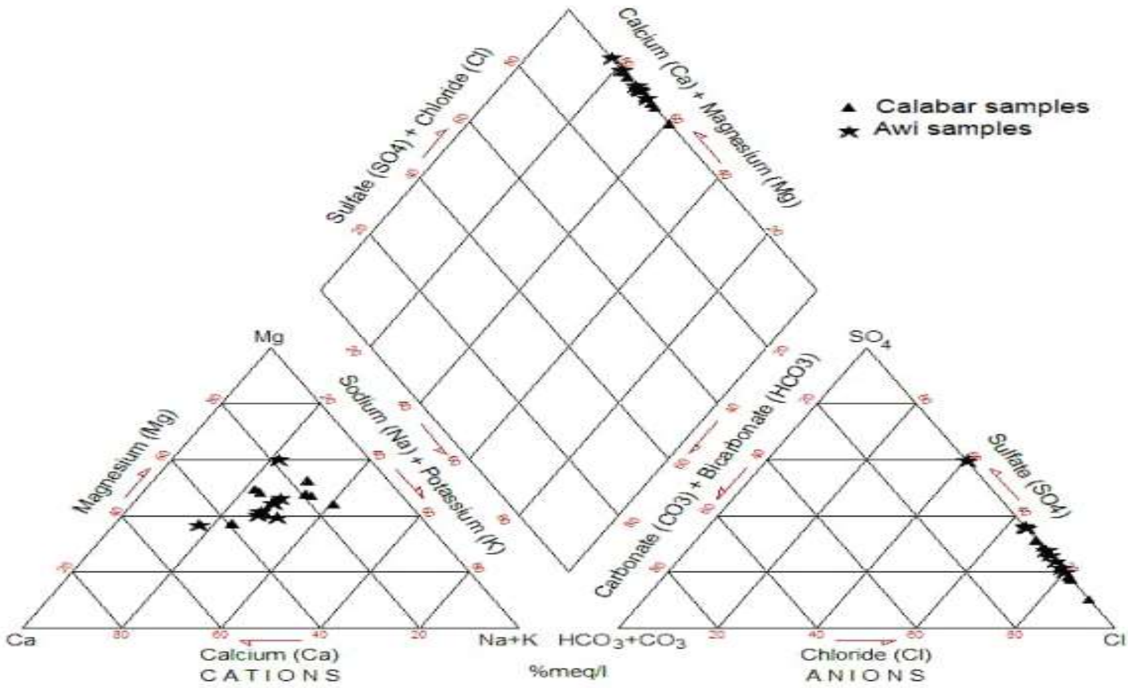

Fig.6: Piper plot of A Calabar and Awi

Geoelectrical parameter analysis of VES data

The geoelectric soundings in Calabar reveals typical sedimentary successions dominated by HK, KH, HA, KQ, and AK curve types. The profiles depict 4 to 5 geoelectric layers of Topsoil/Compacted sand, Clayey sand/Clay, Gravelly coarse-sand. Resistivities vary widely depending on surface organic matter and moisture. Clayey sand/Clay, Low-resistivity intermediate layers acts as semi-pervious horizons. Gravelly coarse-sand (Aquifer Zone), Saturated, high-resistivity layers up to 14,495 Ωm at the depths ranging from (1.91 – 42.9) m. The gravelly sand represents the primary porous media aquifer system in the Coastal Plain Sands. In contrast, the soundings in Awi reveal typical crystalline basement geoelectric sections types of KH, KQ, QQ, as shown in Fig. 4. The basement structure exhibits 3 to 6 distinct geoelectric layers, which consist of Overburden (Clayey/Lateritic Sand), fresh bedrock and weathered/fractured bedrock with moderately low resistivities ranging from (14.4 to 347) Ωm, indicating intense chemical weathering and clay formation. The weathered and fracture bedrock layer acts as a primary groundwater storage reservoir due to high weathered-state porosity. Its high clay content limits hydraulic conductivity. The fractured bedrock (Saprock) marked by medium-to-high resistivity zones indicating secondary jointing and tectonic fracturing. The deep fractured zones, particularly in VES 11, reaching depths of 49.8m, and VES 14 (85.8)m respectively. This formation serves as highly permeable which depicts the main water-yielding targets terrain.

Physical and Chemical parameters

The analytical results for the physical and chemical parameters of both terrains are summarized in the Tables 3 and 4, and compared to WHO (2011) guidelines. The evaluation of Awi setting is characterized by slightly acidic conditions of pH < 5.85, which is typical for crystalline basement water where organic acids and carbon dioxide in infiltrating rainwater trigger silicate hydrolysis. The EC and TDS in both areas contain fresh groundwater (TDS < 500 mg/l). However, groundwater in Calabar exhibits significantly higher mean ionic activities, with EC of 112.33 µS/cm, compared with groundwater in Awi, with EC value of 84.55 µS/cm, indicating enhanced rock-water interaction and saline-air influence in the coastal sedimentary aquifer. Calcium and Magnesium concentrations in both terrains exceed the WHO standard. The highest concentrations occur at locations L3 and L5 in Calabar, and L15 and L19 in Awi, indicating permanent hardness that can cause scale formation in domestic water networks. Widespread geogenic iron enrichment is observed in both aquifer systems. In Awi, iron concentrations peak at 5.18 mg/l at L14, due to the leaching of ferromagnesian minerals from local amphibolites. In Calabar, iron concentrations at L5 reach up to 3.87 mg/l, driven by acidic leaching of ferruginous minerals within the Coastal Plain Sands. This enrichment indicates significant anthropogenic inputs, including domestic sewage leaks, poor sanitary well constructions, and agricultural fertilizer runoff.

From the Pearson correlation analysis, the Calabar sedimentary aquifer shows a strong positive correlation for pH with EC (r = 0.587), Salinity (r = 0.888), and TDS (r = 0.580), indicating ~~the~~ carbonate weathering and localized salt concentrations. However, a high Na-Cl correlation (r = 0.981) ~~was~~ also depicts strong halite dissolution/sea-spray mixing source. Conversely, calcium is negatively correlated with pH (r = -0.669) and TDS (r = -0.578), suggesting precipitation of carbonate minerals under highly alkaline conditions.

In the Awi metamorphic aquifer, pH was strongly correlated with EC (r = 0.736) and TDS (r = 0.725). EC shows high correlation with Magnesium (r = 0.816), Sodium (r = 0.597), and Chloride (r = 0.588). The strong enrichment of Mg^{2+} signified that silicate weathering of ferromagnesian minerals in the amphibolite units serves as the primary driver of regional geogenic mineralization.

The statistical analysis of groundwater in Calabar Municipal shows that the first three principal components (PC 1, PC 2 and PC 3) constitute 96.73% of the total variance in the result of the water chemistry. PC 1 (83.1%) exhibits high loadings for EC, TDS, and HCO3, representing mineral dissolution and rock-water weathering. PC2 (9.7%) has high loadings for Cl and Na, pointing to cation exchange or saline aerosol inputs. PC3 (3.9%) dominated by NO3, reflects anthropogenic pollution. In Awi, the first three principal components account for 90.41% of the total variance. PC1 (53.34%) and PC2 (24.72%) show high loadings for EC, TDS, HCO_{3-}, and Mg^{2+}, reflecting silicate weathering of amphibolite minerals. PC3 (12.35%) is dominated by NO_3^- and Ca^{2+}, representing mixed signatures of human fecal contamination and calcium-bearing plagioclase dissolution.

Water Quality Index

The Water Quality Index (WQI) was determined using the concentrations of various ions Sodium (Na^+), Potassium (K^+), Calcium (Ca^{2+}), Magnesium (Mg^{2+}), Chloride (Cl^-), Sulphate (SO_4^{2-}), Bicarbonate (HCO^-), Nitrate (NO^-), and Iron (Fe), considered in the area of Calabar and Awi. The result reveals the water quality status of the study as shown in Table 5 All the water samples within the two geologic settings have WQI values > 300, classifying the water unsuitable for direct consumption without proper treatment before any use. The~~se~~ high values most reliably resulted primarily from high concentrations of parameters such as calcium (Ca^{2+}), magnesium (Mg^{2+}), Nitrate (NO_3^-) and iron (Fe^{2+}), which exceed WHO permissible limits. The consistently high WQI values across all location underscore the urgent need for groundwater treatment and continuous monitoring to safeguard public health and environmental sustainability

Irrigation Suitability

Irrigation suitability analysis revealed a significant divergence between SAR and MAR hazard indices as summarized in Table 6. The SAR values across both settings are < 3, indicating a low sodium hazard. In contrast, the MAR values present a critical hazardous score in Calabar, ranging from 48.86-76.47 %, while Awi scores ranged from 44.18 -76.37 %. Except for locations L2 in Calabar and L15 in Awi, the MAR values for all the water samples exceed~~s~~ the critical threshold of 50 %. Notwithstanding, the long-term irrigation with a magnesium-enriched groundwater will degrade the soil structure, cause clay dispersion, lower soil infiltration capacity, and reduce crop yields.

Gibb and Piper Plots

The Gibbs diagrams clarify the evolutionary lifecycle of groundwater systems: In the Awi crystalline aquifers, the samples closely clustered within the precipitation dominance field, as shown in Fig. 5. TDS levels were exceptionally low (< 60 mg/L), with cationic weight ratios ranging between 0.4 and 0.6. This indicates that terrain chemistry of Awi is dominated by atmospheric precipitation recharge and rapid flushing. Samples from the Calabar sedimentary display a broader distribution. They transit from the precipitation zone into the rock-water interaction field. TDS values are higher and show greater variability up to 127.4mg/L, indicating longer subsurface residence times that allow for the chemical dissolution of sedimentary matrix minerals.

Piper diagram project major ions classifications of Ca-Mg-Cl-SO4 types. As shown on Fig.6, both aquifers are dominated by permanent (non-carbonate) hardness and highly soluble sulfate and chloride salts, rather than standard calcium bicarbonate recharge facies.

CONCLUSION

This integrated investigation provides a clear comparative evaluation of groundwater potential, chemical evolution, and quality limitations between the sedimentary Coastal Plain Sands of Calabar and the metamorphic Basement Complex of Awi. The Calabar aquifers are porous, unconfined gravel and sand units located at shallow-to-medium depths of 1.91-42.9 m. The crystalline aquifers of Awi are structurally controlled, relying on weathered and secondary fractures up to 6 extending geoelectric layers of 144.7m depth. Groundwaters in both settings are fresh with TDS < 500 mg/l, but severe geogenic and anthropogenic limitations are present. A severe geogenic iron of 5.18mg/l in Awi, and 3.87mg/l in Calabar. There are elevated nitrate concentrations > 50 mg/l and high WQI scores across all the sampled points. These conditions render the groundwater from both terrains unsuitable for direct consumption without proper treatment. Low SAR values indicate a low sodium risk. However elevated MAR scores > 50 % across almost all the wells poses a long-term threat of soil dispersion, alkalization, and reduced infiltration capacity. The Aquifer evolution analysis from Gibb's Plot shows an immature, precipitation-dominated evolutionary stage, in groundwater from the Awi terrain.

In Calabar, a more mature stages transitioning into rock-water interaction were depicted. Both terrains are dominated by the hard Ca-Mg-Cl-SO_4 geochemical facies. This depicts a highly mineralized environment dominated by permanent hardness and the presence of high-solubility salts formations.

REFERENCES:

Abubakar, Y. I, and Yola, L. A., 2012. Geoelectrical Investigation of Groundwater Potential of DawakinTofa Local Government Area of Kano State, Nigeria. American International Journal of Contemporary Research, 2(9), 188-197.

Amah, E. A., 2007. Geophysical and pumping test analyses of groundwater resources of Calabar and its environs. Unpublished Ph.D thesis of the Department of Geology, University of Calabar, 214p.

Amah, E. A., Ugbaja, A. N., and Esu, E. O., 2012. Evaluation of groundwater potentials of the Calabar coastal aquifers. Journal of Geography and Geology, 4(3), 130–139.

Doherty, P., 2017. Global water security and the role of groundwater. Springer Publishing.

Edet A. E, Nganje T. N, Ukpong A. J, Ekwere A.S., 2011. Groundwater chemistry and quality of Nigeria: a status review. African Journal of Environmental Science and Technology 5(13):1152–1169

Ekwueme, B. N., and Okoro, A. U., 2019. Petrology of intrusive rocks of Oban Massif, Southeastern Nigeria. Global Journal of Geological Sciences, 18, 45–59.

Federal Ministry of Water Resources, 2016. National Water Resources Master Plan: Strategy for Water Sector Development. Abuja, Nigeria: Author.

Haritash, A. K., Gaur, S., and Garg, S., 2016. Assessment of water quality and suitability analysis of River Ganga in Rishikesh, India. Applied Water Science, 6(4), 383–392.

Hem, J. D., 1985. Study and interpretation of the chemical characteristics of natural water, 3d Ed., 2254. U.S. Geological Survey Water-Supply Paper, 264p.

Ikechukwu, O. L., and Ogbaji, A., 2019. Groundwater quality assessment in the coastal sedimentary area of Cross River State, Nigeria. International Journal of Environmental Science and Technology, 16(10), 6149–6160.

Jimoh, M. O., Opawale, G. T., Ejepu, J. S., Abdullahi, S., and Agbasi, O. E., 2023. Investigation of Groundwater Potential Using Geological, Hydrogeological and Geophysical Methods in Federal University of Technology, Minna, Bosso Campus, North Central, Nigeria. Hydro Research, 6, 255–268.

Oden, M. I., Ogar, A. M., and Ukwang, E. E., 2019. Petrology and geotechnic setting of the basement comple rocks around Ogoja, South-Eastern Nigeria. International Journal of Geological and Earth Sciences, 5(2), 1-13.

Oguama, V. N., Ohanu, B. A., and Ukaegbu, V. U., 2019. Geoelectric investigation of aquifer characteristics in parts of Imo River basin, Southeastern Nigeria. Journal of African Earth Sciences, 150, 124-135.

Ojo, O. T., Chiaka, I. J., and Nwokeabi, C. N., 2024. Integrated geophysical and GIS approaches for groundwater potential assessment: a case study of Aladja, Delta State, Nigeria. Water Practice and Technology, 19(10), 4282–4295.

Okorobia, E. M., Uko, E. D., Bright, A., and Davies, O. A., 2020. Delineation of Concentration of Ferruginous Minerals in Aquifers in Yenagoa, Bayelsa State, Nigeria, Using Geoelectric Vertical Electrical Sounding (VES) and Physicochemical Techniques. Earth Sciences Malaysia (ESMY), 4(2), 90-101.

Olim, D. M., Afu, S. M., and Akpa, E. A., 2020. Physicochemical properties of wetland soils developed on basement complex and coastal plain sands in Cross River State, Nigeria. Colloquia SSSN, 44, 441–446.

Omosuyi, G. O., 2010. Geo-electric Assessment of Groundwater Prospect and Vulneability of Overburden Aquifer at Idanre, Southwestern Nigeria. Ozean Journal of Applied Sciences, 3(1), 19-28.

Paliwal, K.V., 1972. Irrigation with saline water, Monogram no. 2 (New series). New Delhi.

Patil, P. N., Sawant, D. V., and Deshmukh, R. N., 2012. Physico-chemical parameters for testing of water – A review. International Journal of Environmental Sciences, 3(3), 1194-1205.

Reeve, R. C., Bower, C. A., Brooks, R. H., Gwchwend, F. B., 1954. A comparison of the effects of exchangeable sodium and potassium upon the physical condition of soils. Soil Science Society of American Journal. 18, 130–132.

Thomas, E. O., 2023. Evaluation of groundwater quality using multivariate, parametric and non-parametric statistics, and GWQI in Ibadan, Nigeria. Water Science, 37(1), 117-130.

World Health Organization (WHO), 2011. Guidelines for drinking-water quality (4th ed.). Geneva: WHO Press.